

Discovery of Sodium and Potassium Vapor in the Atmosphere of the Moon

A. E. POTTER AND T. H. MORGAN

Spectra of the region just above the bright limb of the Moon show weak emission features that are attributed to resonant scattering of sunlight from sodium and potassium vapor in the lunar atmosphere. The maximum omnidirectional emission flux above the bright limb is 3.8 ± 0.4 kilorayleighs for sodium and 1.8 ± 0.4 kilorayleighs for potassium. The zenith column densities above the subsolar point are estimated to be $8 \pm 3 \times 10^8$ atoms cm^{-2} for sodium and $1.4 \pm 0.3 \times 10^8$ atoms cm^{-2} for potassium. Corresponding surface densities are 67 ± 12 atoms cm^{-3} and 15 ± 3 atoms cm^{-3} , respectively. The scale height for the sodium atmosphere is 120 ± 42 kilometers, and for potassium 90 ± 20 kilometers, which implies that the effective temperature of the sodium and potassium is close to the lunar surface temperature. The sodium density at the south polar region was found to be similar to that at the subsolar point, indicating widespread distribution of sodium vapor over the lunar surface. The ratio of the density of sodium to the density of potassium is (6 ± 3) to 1, which is close to the sodium to potassium ratio in the lunar surface, suggesting that the atmosphere originates from the vaporization of surface minerals.

DESPITE THE ATMOSPHERIC MEASUREMENTS PERFORMED during the Apollo missions, we know remarkably little about the atmosphere of the Moon. Pressure gauges were deployed on the lunar surface, and detected a total density of the order of 10^6 atoms cm^{-3} at the subsolar point (1). A far-ultraviolet spectrometer flown on the Apollo 17 orbiter (2) was used to look for sunlight scattered from atmospheric gases having resonance emission lines in the vacuum ultraviolet. No emissions were found. However, these measurements did set upper limits for a number of possible atmospheric gases, such as argon, oxygen, carbon monoxide, and hydrogen, at levels well below the total density measured by the pressure gauges. A mass spectrometer on the lunar surface was used in an effort to determine the composition of the atmosphere (3). Argon, neon, and helium were detected in the nightside atmosphere, and there was some evidence for the presence of methane and ammonia at sunrise. Unfortunately, daytime measurements were rendered useless by contamination from the lander vehicle. The composition of the dayside atmosphere remains unknown. It has been suggested that the major constituent of the dayside atmosphere might be carbon dioxide (4), but that appears to conflict with the upper limit on carbon monoxide established by

A. E. Potter is chief of the Space Science Branch, Solar System Division, NASA Johnson Space Center, Houston, TX 77058. T. H. Morgan is a National Research Council Senior Associate assigned to Space Science Branch, Solar System Exploration Division, NASA Johnson Space Center, Houston, TX 77058.

ultraviolet spectroscopy. These few facts represent the sum of existing data concerning the lunar atmosphere, which is properly called an exosphere, because gas-phase collisions are negligible.

Discovery of the sodium and potassium atmosphere of Mercury (5, 6) led to the examination of processes that could produce the observed sodium and potassium vapors (7). It was concluded that impact vaporization from the infall of meteoroids, solar wind sputtering, and photosputtering could all generate sodium and potassium vapor in varying degrees from the planetary surface. These concepts were extended to calculate the rate of generation of sodium vapor from the surface of the Moon (8), with the result that it appeared possible that sufficient sodium might be released to generate an atmosphere that could be observed by resonance scattering of sunlight from the sodium vapor. We have searched for this atmosphere by means of high resolution spectroscopy, and report here the discovery of both sodium and potassium in the atmosphere of the Moon. The capability to map and monitor the sodium and potassium exospheres of the Moon by means of ground-based telescopes should lead to a significantly better understanding of the lunar atmosphere, as well as the similar atmosphere observed for Mercury.

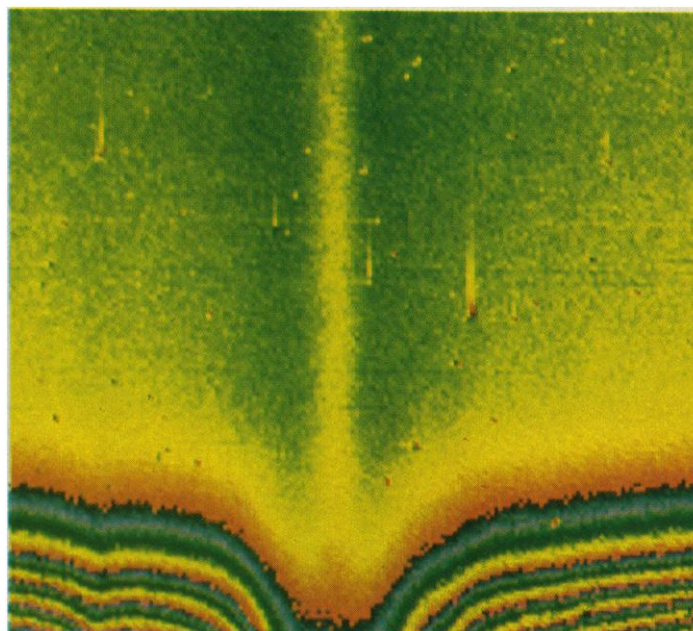


Fig. 1. An image of the subsolar limb of the Moon in the spectral region of the sodium D_2 line at 5889.7 \AA . The length of the vertical axis is 28 arc sec ($0.14 \text{ arc sec per pixel}$) and the length of the horizontal axis is 2.16 \AA ($5.4 \text{ m\AA per pixel}$). The edge of the Moon is at the bottom. Above the lunar surface, centered on the solar sodium Fraunhofer absorption minimum, there is seen a weak emission line that extends to the top of the image. The line is sodium resonance radiation, produced from scattering of sunlight by sodium vapor in the lunar atmosphere.

Emission line spectra. Preliminary observations of the Moon at the 7699 Å resonance line of potassium were made on 8 February 1987 with the 2.7-m telescope at the McDonald Observatory. A positive, although noisy, indication was found for the presence of potassium emission above the lunar surface. A more extensive series of observations was made between 12 and 15 January 1988 at both the McDonald Observatory and the National Solar Observatory (NSO) at Kitt Peak, and a number of excellent spectra were obtained at the wavelengths of both sodium and potassium resonance lines. The observations are summarized in Table 1. In all cases, emission was observed above the limb of the Moon. The emission was not dependent on the elevation of the Sun, nor on the elevation and zenith of the Moon during the observations.

Observations at the McDonald Observatory were made with the coude echelle spectrograph in single-pass mode. The spectra were recorded with an 800 pixel by 800 pixel charge-coupled device (CCD), so as to give images with one spectral and one spatial dimension. An image of the subsolar limb of the Moon measured on 13 February in the spectral region of the sodium D₂ line at 5889.7 Å is shown in Fig. 1. Each vertical element in the figure corresponds to 0.14 arc sec angular distance, and each horizontal element corresponds to 5.4 mÅ in the spectral dimension. (Image jitter reduced the spatial resolution to an effective value of about 2.2 arc sec, and the spectrograph optics were such that the effective spectral resolution was 22 mÅ.) Spectra of sunlight reflected from the lunar surface appear at the bottom of the figure. The color bands on the lunar spectra are contour lines of intensity, with 256 levels in each band. Above the lunar surface, centered on the solar sodium Fraunhofer absorption minimum, there is seen a weak emission line that extends to the top of the image. The line is sodium resonance radiation, produced from scattering of sunlight by sodium vapor in the lunar atmosphere.

Observations of sodium emission were also made with the main beam and the stellar spectrograph on the McMath Solar telescope at NSO. The image slicer at the entrance aperture of this spectrograph provides a 5 arc sec by 5 arc sec array of 45 spectra. The image slicer was positioned over the limb of the Moon, so as to obtain spectra from both the lunar surface and the region immediately above it. The spectrograph was operated at a resolution of about 100 mÅ, which meant that the sodium emission line was not resolved in the solar Fraunhofer absorption line, but rather "filled in" the line. The spatial span of only 5 arc sec meant that none of the spectra were entirely free of light from the lunar surface, because seeing and image jitter and wander caused the effective seeing to be about 2.5 arc sec. Useful measurements were made of the subsolar limb and of the south polar limb. In both cases, "filling in" of the Fraunhofer line increased significantly as the distance away from the lunar surface increased. The strong Fraunhofer line at 5892.8 Å, which lies between the two sodium D lines, did not show any evidence of "filling in" in any of the spectra, which showed that the "filling in" of the sodium line was not the result of scattered light in the optical system. The limited spatial extent of these measurements did not provide any information on scale height of the emission, but did demonstrate that the emission could be detected at lunar locations other than the subsolar point.

The possibility that the emissions observed were from a terrestrial source was examined carefully, because there are several possible terrestrial origins for sodium and potassium emissions. These include sodium emission in the nightglow, sodium and potassium emissions in the twilight glow, and scattered light from low-pressure sodium vapor lamps in the cities of Alpine and Tucson.

First, the nightglow: The spectra of a number of standard stars, Venus, and the asteroid Vesta were recorded for a large range of air masses, times of the night, and exposures during the McDonald

Table 1. Journal of observations of lunar sodium and potassium.

| Run | Date and time open (UT) | Wavelength and exposure time | Moon | | Sun | |
|-----|-------------------------|------------------------------|-----------------------------------|----------------------------|-----------------------|----------------------|
| | | | Azimuth begin/end (degrees) | Zenith begin/end (degrees) | Azimuth end (degrees) | Zenith end (degrees) |
| | | | <i>McDonald Observatory</i> | | | |
| 15 | 8 February 1987 0221 | 7699 Å 30 minutes | | 26/19 | 257 | 98 |
| 8 | 12 January 1988 1045 | 5889 Å 30 minutes | 138/146 | 52/48 | 96 | 123 |
| 9 | 12 January 1988 1137 | 7699 Å 30 minutes | 152/162 | 46/44 | 102 | 112 |
| 10 | 12 January 1988 1216 | 7699 Å 30 minutes | 165/175 | 44/43 | 106 | 104 |
| 11 | 12 January 1988 1251 | 7699 Å 30 minutes | 177/188 | 43/43 | 110 | 97 |
| 12 | 12 January 1988 1322 | 7699 Å 30 minutes | 188/198 | 43/45 | 114 | 91 |
| 27 | 13 January 1988 1054 | 5889 Å 60 minutes | 134/148 | 62/54 | 101 | 115 |
| 28 | 13 January 1988 1157 | 5889 Å 60 minutes | 148/165 | 54/49 | 107 | 102 |
| 52 | 14 January 1988 1134 | 5889 Å 60 minutes | 135/148 | 68/60 | 105 | 107 |
| 88 | 15 January 1988 1223 | 5889 Å 30 minutes | 137/143 | 72/68 | 105 | 102 |
| 90 | 15 January 1988 1306 | 6665 Å 30 minutes | 145/152 | 66/63 | 112 | 94 |
| | | | <i>National Solar Observatory</i> | | | |
| 17 | 13 January 1988 1108 | 5889 Å 10 minutes | 132/133 | 66/64 | 91 | 131 |
| 18 | 13 January 1988 1134 | 5889 Å 10 minutes | 137/139 | 62/60 | 94 | 125 |

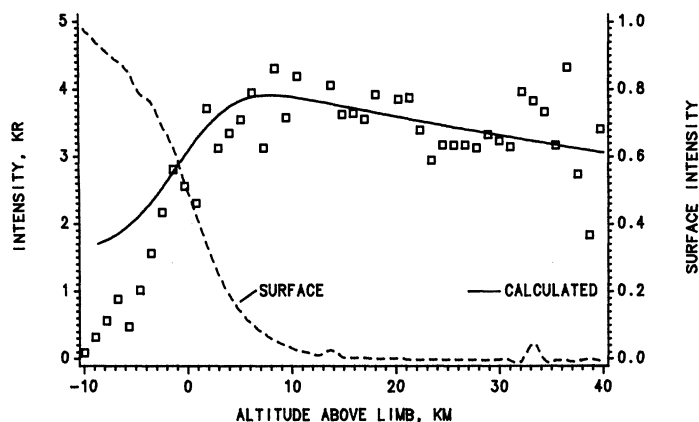


Fig. 2. The omnidirectional emission rate owing to sodium above the bright limb at the subsolar point. These data are derived from the image shown in Fig. 1. The solid line was calculated for a subsolar point density of 67 atoms cm^{-3} , and a scale height of 120 km convolved with 2.2 arc sec seeing (13 January 1988, McDonald Observatory).

Observatory run. The Vesta observation totaled more than 2 hours. In no case was there any evidence of a sodium emission line, which shows that the sodium nightglow intensity was below the threshold of detection in these measurements.

Second, the twilight glow: In order to excite the twilight glow, the elevation of the Sun might be higher than 12 degrees below the horizon, which corresponds to sunrise at 100 km. As shown in Table 1, all of the sodium observations were taken when mesospheric sodium emission could not have been present, that is, at times when the sun was more than 12 degrees below the horizon. This is not the case for potassium, where two of the four observations were made after sunrise at 100 km. However, there is no significant difference between the observations made before and after a 100-km sunrise, so that the twilight potassium emission was evidently below the threshold of detection.

Third, light contamination from sodium vapor lamps used for street lighting: The number of low-pressure sodium lamps in the nearest substantial human settlement, the city of Alpine (50 km ESE of the observatory), was determined to be 170 units each of 4800 lumens. On the basis of the technical information available as to light output from such lamps (9, 10), and assuming that half the emitted photons are scattered into the atmosphere, the intensity of sodium radiation in the field of view of the telescope was estimated to be about 20 rayleighs [1 rayleigh = 10^6 photons cm^{-2} (column) sec^{-1}] for the worst case. It will be shown later that the observed sodium emission is several kilorayleighs, so that contamination of the McDonald observations by street lights was not significant. Similar considerations apply to the NSO observations.

Analysis of spectra. The spectra were calibrated in terms of photon flux with the lunar reflectance spectra present in each exposure used as a standard source. If A_i is the integrated number of counts under the emission line in the i th spectral row after flat fielding, bias subtraction, and subtraction of scattered continuum, and A_c is the total number of counts in the same spectral range from the bright surface of the Moon, then the ratio of the surface brightness of the emission line, Φ_{ei} , to the surface brightness of the solar continuum reflected from the lunar surface, Φ_c , is given by

$$\Phi_{ei}/\Phi_c = A_i/A_c \quad (1)$$

where the “continuum” here is actually at the bottom of the broad Fraunhofer line in the solar spectrum. (The Doppler shift of the resonance lines of sodium and potassium in the lunar atmosphere relative to the solar Fraunhofer line ranges from zero at full and new

moon to about 25 mÅ at first and third quarter. Consequently, the sunlight available for resonant scattering lies near the bottom of the Fraunhofer lines.)

The bidirectional reflectance r_h is defined as the ratio of the radiant power received per unit area per unit solid angle from a specific direction to the radiant power per unit area from a source of collimated light that illuminates the surface from a specific direction. Hence,

$$\Phi_c = r_h(\pi F)_c \quad (2)$$

where r_h is the Hapke bidirectional reflectance function for the lunar surface for the phase angle of the Moon at the time of the observation and for the luminance coordinates of the site (11), and $(\pi F)_c$ is the incident solar flux per unit area. Solving for the surface brightness of the emission, and multiplying by 4π to obtain the omnidirectional flux, we obtain

$$(4\pi\Phi_{ei}) = (A_i/A_c)4\pi r_h(\pi F)_c \quad (3)$$

The “equivalent width” of the emission is given by

$$\delta\lambda = (4\pi\Phi_{ei})/(\pi F)_c = (A_i/A_c)4\pi r_h \quad (4)$$

which has units of equivalent width if $(\pi F)_c$ is in photons $\text{cm}^{-2} \text{sec}^{-1} \text{mÅ}^{-1}$. This “equivalent width” represents the total number of photons scattered out of the solar spectrum by the metal vapor atoms. Under the assumption that the region of line formation is optically thin, this number is directly proportional to the zenith column density above the bright limb. The total light flux in units of kilorayleighs can be obtained by multiplying the “equivalent width” by the solar flux in units of kilorayleighs (kR) per mÅ at the resonance line wavelength. For sodium, the result is

$$(4\pi\Phi_{ei}) = 3.1 \text{ kR (mÅ)}^{-1} \delta\lambda \quad (5)$$

For potassium the same analysis yields

$$(4\pi\Phi_{ei}) = 9.8 \text{ kR (mÅ)}^{-1} \delta\lambda \quad (6)$$

The essential data elements needed to calculate the flux of sodium and potassium radiation are seen to be (i) the integrated number of counts under the emission line, (ii) the integrated number of counts under the lunar reflectance continuum spectrum at the position of the emission line, and (iii) the bidirectional reflectance of the lunar surface. The integrated number of counts under the emission line was obtained by interpolating the Fraunhofer line profile from both sides of the emission line to obtain a baseline underneath the emission peak, then subtracting this baseline from the spectrum to obtain the emission line profile, which was then integrated. This procedure was satisfactory away from the lunar surface, where the emission line was the dominant spectral feature. The standard deviation for measurements above the bright limb was 0.4 kR. However, on the lunar surface, where the emission line was only a few percent of the signal, the results were uncertain by a substantial amount. The lunar reflectance continuum intensity under the emission line was determined from a spectrum of the bright lunar surface. First, the intensity of the continuum at a spectral position far removed from the Fraunhofer line was measured. This value was then multiplied by the fractional depth of the Fraunhofer line to obtain the continuum level under the emission line. The lunar bidirectional reflectance was obtained from published values (11).

Thus the omnidirectional emission rate of sodium as a function of height above the bright limb at the bright limb at the subsolar point (Fig. 2) was derived from the image (Fig. 1). The location of the lunar surface (the zero point on the distance scale) was assumed to be the point at which the intensity of the continuum radiation from the lunar surface dropped to half of its maximum value. The peak sodium emission away from the lunar surface was 3.8 ± 0.4 kR. The

intensity appears to decrease rapidly on the lunar surface. However, values of the emission intensity measured on the lunar surface are very uncertain, because the sodium emission intensity is only a few percent or less of the continuum intensity in this region. A solid line labeled "calculated" is drawn through the data. The calculations leading to this line will be discussed later.

The omnidirectional emission rate resulting from potassium as a function of height above the bright limb at the subsolar point (Fig. 3) was derived from the average of the last three potassium measurements performed on 12 January 1988 at McDonald Observatory. The potassium emission away from the lunar surface averages about 1.5 ± 0.4 kR. As for the case of sodium, the values calculated over the lunar surface are subject to considerable uncertainty. As before, a solid line labeled "calculated" is drawn through the data, and will be discussed later.

The omnidirectional emission rate resulting from sodium was also derived from the observations with the stellar spectrograph at the McMath Solar Observatory (Fig. 4). As noted previously, the angular distance covered in this measurement was only 5 arc sec, so that only a limited height range was covered. Data for both the subsolar point and for the south polar region are plotted, and mean lines have been drawn through each set of data. It is evident that there is little difference between the two data sets, indicating that the sodium emission is widespread across the Moon, with little variation in abundance. The intensity of the emission at the lunar surface (0-km altitude) determined from these data is about 1.5 kR, which is significantly less than the value of about 2.5 kR at the same point calculated from the McDonald Observatory data. The difference is thought to result from systematic underestimation of the intensity of the sodium emission, on account of the lower resolution of the data from the stellar spectrograph, such that the emission line was unresolved.

Analysis of the emission spectra. The column and surface densities, and the scale heights for sodium and potassium, can be determined from the observed distributions of emission as follows:

The flux of radiation observed at some point h above the bright limb as observed from Earth is (12)

$$(4\pi\Phi_\epsilon)_h = g \int N(r') ds' \quad (7)$$

where g is the photon scattering coefficient, s' is the distance along the line of sight measured from the point of closest approach to the Moon, r' is the distance from the center of the Moon to the line of sight s' , and is equal to $[(r_0 + h)^2 + s'^2]^{1/2}$, r_0 is the radius of the Moon, and $N(r')$ is the local density of sodium in atoms cm^{-3} . The integral, which is the tangentially integrated column density, can be calculated numerically if $N(r')$ is known. Here we shall assume that

$$N(r') = N(r_0) \exp[-(r' - r_0)/H] \quad (8)$$

where H is the scale height and $N(r_0)$ is the density at the surface. Then

$$(4\pi\Phi_\epsilon)_h = gn_0 \int \exp[-(r' - r_0)/H] ds'/H \quad (9)$$

where n_0 is the zenith column density, and the integral is now dimensionless as we have changed the variable of integration to s'/H . The relative variation of the intensity above the bright limb is entirely contained in the integral. If there were no effect of atmospheric turbulence and telescope guiding errors on the image, it would simply remain to calculate these quantities for a suite of n_0 and H combinations, and make the best possible fit to the data. However, because the image is blurred by these effects, the intensities must be convolved with a seeing spread function. This function was assumed to be a Gaussian distribution, and its parameters were

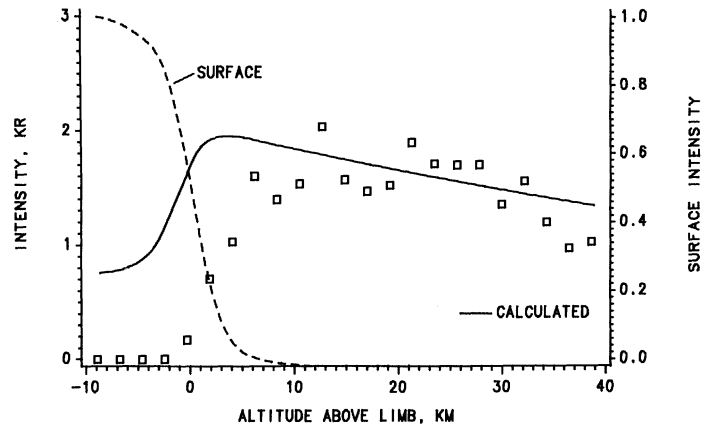


Fig. 3. The omnidirectional emission rate owing to potassium above the bright limb at the subsolar point. The solid line was calculated for a subsolar point density of 15 atoms cm^{-3} and a scale height of 90 km, convolved with 1.1 arc sec seeing (12 January 1988, McDonald Observatory).

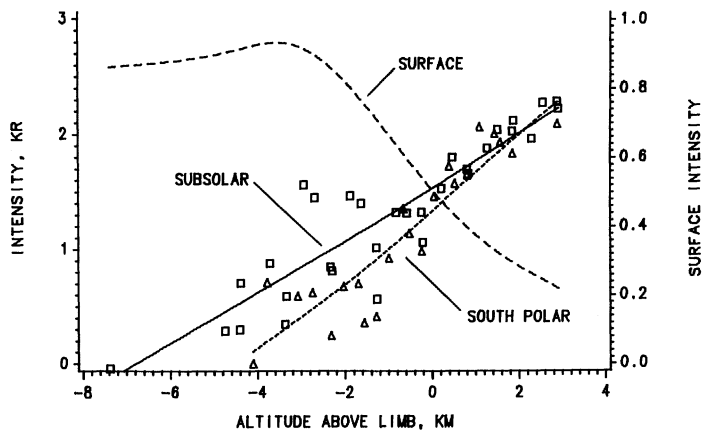


Fig. 4. The omnidirectional emission rate owing to sodium above both the subsolar point and the south pole (13 January 1988, National Solar Observatory).

determined from the distribution of intensity of the continuum radiation from the bright limb of the Moon. Once the seeing function was known, the variation of intensity with respect to height above the bright limb was calculated for a suite of scale heights and column densities and the results compared to the observed intensities above the bright limb.

The standard deviations for scale height and surface density were estimated from the portion of the data at altitudes above the lunar surface, where the dependence of intensity with altitude is approximately linear. Data in this region were fitted to a linearized approximation to the exact equation (9), and standard deviations for scale height and surface density were calculated from a least-squares fit to the line.

The "calculated" solid line shown in Fig. 2 is our best fit to the sodium distribution data. This line corresponds to a column density of $8 \pm 3 \times 10^8 \text{ atoms cm}^{-2}$ and a scale height of $120 \pm 42 \text{ km}$. The corresponding density at the base of the column is $67 \pm 12 \text{ atoms cm}^{-3}$. The calculated intensities do not match the observed intensities on the bright limb proper. We believe this to be the result of the large uncertainties of measuring the weak sodium emission in the presence of the large lunar reflection intensity.

If the velocity distribution function of the sodium atoms were Maxwellian, and the atmosphere in hydrostatic equilibrium, a 120-km scale height would be associated with a kinetic temperature of 540 K and a mean velocity of 0.6 km sec^{-1} . The effective broaden-

ing of the line when fine structure is included would be approximately 40 mÅ. The measured full width at half-maximum of the emission line was found to be 42 mÅ, which supports the finding of a low kinetic temperature for the sodium atoms. Although the velocity distribution is likely not to be perfectly Maxwellian (13), the difference is not likely to be great enough to modify this conclusion.

The “calculated” solid line shown in Fig. 3 is our best fit to the potassium distribution data, derived in the same way as for the sodium data. This line corresponds to a column density of $1.4 \pm 0.3 \times 10^8$ atoms cm^{-2} and a scale height of 90 ± 20 km. The corresponding density at the base of the column is 15 ± 3 atoms cm^{-3} . As in the case of sodium, the calculated emission rates do not match the emission rates on the bright limb proper. The ratio of the column density of sodium to that of potassium found from this analysis is (6 ± 3) to 1. The ratio of the scale height of potassium to the scale height of sodium is 1.3 ± 0.4 . If the exospheric distribution were simply exponential and the temperature of each species were the same the ratio would be 1.7, which is within the error bar. If further measurements show this difference to be real, then a more complex model of the exosphere will be required.

Sources and sinks of sodium and potassium. Two recognized avenues for loss of sodium from the lunar atmosphere are (i) thermal escape and (ii) photo-ionization followed by loss by the Manka-Michel mechanism (14). The lifetime against photo-ionization of sodium at 1 AU is 5.6×10^4 sec, much shorter than the lifetime against loss by thermal escape. Consequently, photo-ionization could be the rate-determining process for loss of sodium. If we take the average lifetime of a sodium atom in the atmosphere, τ , to be the photo-ionization lifetime, then the source rate of sodium, the loss rate of it, and the column density n_0 are related by the equality

$$n_0 = \Sigma\tau \quad (10)$$

where Σ is the supply of new sodium in atoms $\text{cm}^{-2} \text{sec}^{-1}$. From our data, we calculate that the supply of new sodium to the atmosphere must be 1.4×10^4 atoms $\text{cm}^{-2} \text{sec}^{-1}$.

There are at least five possible sources for constituents of the lunar atmosphere: Solar-wind implantation and subsequent release of sodium, solar wind-driven sputtering of sodium, impact-driven vaporization, photon-stimulated desorption, and internal release. Solar-wind implantation can only supply less than 100 atoms $\text{cm}^{-2} \text{sec}^{-1}$ of sodium and so this mechanism can be eliminated. We know of no internal release mechanism likely to produce sodium. The remaining three can all be expected to supply sodium at a rate equal to or greater than 10^4 atoms $\text{cm}^{-2} \text{sec}^{-1}$ (3). [A detailed discussion of these rates is found in (4).] The presence of sodium near the south pole at large local solar zenith angles suggests that impact vaporization might predominate over the other processes, but rapid diffusion from the subsolar point, where the other two processes are dominant, might be sufficient to invalidate this argument.

The possible sources of sodium are also possible sources of potassium. Both sputtering and impact vaporization should supply potassium to the atmosphere of the Moon. No calculations of the yield of potassium ejected by photon-stimulated desorption are available, but there is no reason to think that the process will not eject potassium atoms as well. To a first approximation, then, the ratio, $\Sigma_{\text{potassium}}/\Sigma_{\text{sodium}}$, should equal the ratio of the abundances of the two elements in the regolith. This alone does not mean that the ratio of the observed column densities of sodium and potassium will be equal to the ratio of their abundances in the regolith because the column density is in each case the product of the supply rate and the lifetime. If, however, the lifetimes are approximately the same the ratio of the column densities should be close to the ratio of the regolith abundances. This is what is observed.

Comparison to the exosphere of Mercury. The exosphere of the

Moon invites immediate comparison to the exosphere of Mercury. The differences are notable. Sodium column densities on Mercury approach a few times 10^{11} atoms cm^{-2} , a factor of 200 times that about the Moon (16). The difference is not limited to sodium. Fastie *et al.* (2) reported an upper limit on oxygen in the exosphere of Mercury of 80 atoms cm^{-3} . The revised Mariner 10 results (15) are more than 4×10^4 atoms cm^{-3} . The two dominant species in the atmosphere of Mercury are minor constituents in the atmosphere of the Moon. It has been argued that carbon dioxide is the major constituent of the bright-side atmosphere on the Moon. This is clearly not the case in the atmosphere of Mercury. If the difference were just sodium one could argue that relative abundance differences between the regoliths might play a role (more sodium in the surface layer of Mercury than in that of the Moon), and this may be the case (17), but this argument fails for oxygen. The source rates will certainly be different on the planet (3), but the difference is likely to be closer to 25 than 250. One important difference between the two bodies is the magnetosphere of Mercury. Although a magnetosphere can act to recycle photo-ions, the best studies of the matter (18) argue that it affords an effective loss mechanism for sodium on Mercury, exacerbating the difference.

The sodium to potassium ratio in the Mercury atmosphere is in the range of 80 to 100, whereas in the lunar atmosphere we find a ratio of 6. The lunar ratio apparently reflects the sodium to potassium ratio in the regolith (19), so that it is reasonable to suppose that the same might be true for Mercury. This could mean that the regolith of Mercury is substantially different from that of the Moon, being greatly depleted of potassium.

Conclusions. Spectra of the bright limb of the Moon at both the Fraunhofer sodium D₂ line and the potassium 7699 Å line show weak emission features that are attributed to resonant scattering of sunlight from sodium and potassium vapor above the subsolar point. The omnidirectional emission flux above the bright limb is 3 to 4 kR for sodium and 1 to 2 kR for potassium. The sodium emission extends to the poles, and the zenith column density of sodium above the subsolar point on the bright limb is $8 \pm 3 \times 10^8$ atoms cm^{-2} , while the scale height for the sodium atmosphere is 120 ± 42 km. The zenith column density of potassium above the subsolar point is $1.4 \pm 0.3 \times 10^8$ atoms cm^{-2} , while the scale height is 90 ± 20 km. The ratio of the density of sodium in the lunar atmosphere to the density of potassium is (6 ± 3) to 1, which is close to the sodium to potassium ratio in the lunar surface minerals.

The exosphere of the Moon contrasts markedly with the exosphere of Mercury. Sodium and oxygen, the principal species in the sunlit exosphere of Mercury, are only minor constituents in the exosphere of the Moon. The same physical processes work to evolve sodium on both Mercury and the Moon and the expected rates do not differ by the same magnitude as do the observed column densities. The explanation may lie in the interaction of photo-ions with the magnetosphere of Mercury. The ratio of sodium to potassium on Mercury is in the range of 80 to 100 to 1, markedly greater than the value found for the Moon. Since the lunar ratio appears to reflect the ratio found in the regolith, it is reasonable to suppose the same might be true for Mercury, which implies that the Mercury regolith could be greatly depleted in potassium relative to sodium.

Note added in proof: Tyler *et al.* (20) have confirmed the presence of sodium in the lunar exosphere.

REFERENCES AND NOTES

1. F. S. Johnson, *Rev. Geophys. Space Phys.* **9**, 813 (1971).
2. W. G. Fastie *et al.*, *Science* **182**, 710 (1973).
3. J. H. Hoffman and R. R. Hodges, *Moon* **14**, 159 (1975).
4. R. R. Hodges, *Proc. Lunar Planet. Sci. Conf.* **7**, 493 (1976).

5. A. E. Potter and T. H. Morgan, *Science* **229**, 651 (1985).
6. ———, *Icarus* **67**, 336 (1986).
7. T. H. Morgan, H. A. Zook, A. E. Potter, *ibid.* **75**, 156 (1988).
8. ———, *Proc. Lunar Planet. Sci.* **19**, 676 (1988).
9. J. W. Denneman, *IEE Proc.* **128A**, 397 (1981).
10. There are sixty 5800-lumen high-pressure sodium lamps in use in Alpine, but the spectrum from a high-pressure sodium lamp is strongly self-absorbed near line center. See J. A. J. M. van Vliet and J. J. de Groot, *IEE Proc.* **128A**, 415 (1981).
11. B. W. Hapke, *Icarus* **59**, 41 (1984).
12. J. W. Chamberlain and D. M. Hunten, *Theory of Planetary Atmospheres* (Academic Press, New York, 1987), p. 292.
13. D. E. Shemansky and A. L. Broadfoot, *Rev. Geophys. Space Phys.* **15**, 491 (1977).
14. R. H. Manka and F. C. Michel, *Geochem. Cosmochem. Acta Suppl.* **3**, 2, 1717 (1971).
15. D. M. Hunten, T. H. Morgan, D. E. Shemansky, in *Mercury*, F. Vilas, C. R. Chapman, M. S. Matthews, Eds. (Univ. of Arizona Press, Tucson, in press).
16. A. E. Potter and T. H. Morgan, *Icarus* **71**, 472 (1987).
17. S. R. Taylor, in *Workshop on the Growth of Continental Crust* (Lunar and Planetary Institute, Houston, TX, 1987), pp. 108–110.
18. A. F. Cheng *et al.*, *Icarus* **71**, 430 (1987).
19. R. J. Williams and J. J. Jadwick, *Handbook of Lunar Materials*, Report NASA-RP-1057 (National Aeronautics and Space Administration, Washington, DC, 1980).
20. A. L. Tyler, R. W. H. Kozlowski, D. M. Hunten, *Geophys. Res. Lett.*, in press.
21. We thank D. Doss and C. Opal of the University of Texas McDonald Observatory and B. Graves of the National Solar Observatory for their help in obtaining the observations. This article benefited from discussions with J. Chamberlain and R. Killen of Rice University and with D. Shemansky of the University of Arizona. Both authors are guest observers at the McDonald Observatory of the University of Texas at Austin, TX, and are visiting astronomers at the National Solar Observatory, operated by the Association of Universities for Research in Astronomy, Inc., under contract with the National Science Foundation.

2 May 1988; accepted 8 July 1988

Antisense RNA Directed Against the 3' Noncoding Region Prevents Dormant mRNA Activation in Mouse Oocytes

SIDNEY STRICKLAND,* JOAQUIN HUARTE, DOMINIQUE BELIN, ANNE VASSALLI,†
RICHARD J. RICKLES, JEAN-DOMINIQUE VASSALLI

Primary mouse oocytes contain untranslated stable messenger RNA for tissue plasminogen activator (t-PA). During meiotic maturation, this maternal mRNA undergoes a 3'-polyadenylation, is translated, and is degraded. Injections of maturing oocytes with different antisense RNA's complementary to both coding and noncoding portions of t-PA mRNA all selectively blocked t-PA synthesis. RNA blot analysis of t-PA mRNA in injected, matured oocytes suggested a cleavage of the RNA:RNA hybrid region, yielding a stable 5' portion, and an unstable 3' portion. In primary oocytes, the 3' noncoding region was susceptible to cleavage, while the other portions of the mRNA were blocked from hybrid formation until maturation occurred. Injection of antisense RNA complementary to 103 nucleotides of its extreme 3' untranslated region was sufficient to prevent the polyadenylation, translational activation, and destabilization of t-PA mRNA. These results demonstrate a critical role for the 3' noncoding region of a dormant mRNA in its translational recruitment during meiotic maturation of mouse oocytes.

DURING THE GROWTH PHASE OF OOGENESIS, MESSENGER RNA molecules accumulate that are not translated until after the oocyte enters the final phases of maturation or is fertilized (1). This posttranscriptional regulation allows rapid alterations in protein synthesis as maturation and embryogenesis are initiated. For this process to occur, the dormant mRNA's must have characteristics, such as structural determinants and subcellular location, that permit their selective and timely translational activation.

In mammals, little is known about mRNA recruitment during

meiotic maturation, since specific dormant mRNA's have only recently been identified. The mRNA for tissue plasminogen activator (t-PA) is present in primary (germinal vesicle-containing) mouse oocytes, but the enzyme is not synthesized until resumption of meiosis, in the hours that precede ovulation. The dormant, stable mRNA accumulates during the oocyte's growth phase and is stored in the cytoplasm of the primary oocyte. After resumption of meiosis, the mRNA progressively acquires about 500 adenosine (A) residues at the 3' end, and concomitantly it is translated. Later, this mRNA becomes unstable, so that it is undetectable in fertilized eggs (2, 3). The expression of hypoxanthine phosphoribosyl transferase (HPRT) has similar characteristics in that an increase in enzyme activity during maturation and early embryogenesis may be due to the activation of a maternal mRNA (4), and HPRT mRNA is elongated during oocyte maturation and then degraded after the two-cell stage (5).

Regarding maternal mRNA's in mammals and other species, it is still not known (i) what molecular determinants specify the initial dormancy and then the temporally precise activation, structural alteration, and destabilization; (ii) whether these events are interrelated; and (iii) what roles are played in early development by the products of the genes whose expression is so exquisitely controlled.

Antisense RNA inhibition of gene expression (6) is well suited for addressing these questions in general, and the regulated expression of t-PA in mouse oocytes in particular. The amount of t-PA mRNA

This work was performed while S. Strickland, J. Huarte, A. Vassalli, and J.-D. Vassalli were in the Institute of Histology and Embryology, D. Belin was in the Department of Pathology, University of Geneva Medical School, CH-1211 Geneva 4, Switzerland, and R. J. Rickles was in the Department of Molecular Pharmacology, State University of New York, Stony Brook, NY 11794.

*Permanent address: Department of Molecular Pharmacology, State University of New York, Stony Brook, NY 11794.

†Present address: Department of Biology, Massachusetts Institute of Technology, Cambridge, MA 02139.